67 GHz graphene electro-absorption modulators on silicon with 80 Gb/s C-band and 40 Gb/s O-band NRZ data rates

Matteo Tiberi[1*], Alberto Montanaro[2], Chao Wen[1], Jincan Zhang[1], Marco Romagnoli[3], Vito Sorianello[2] and Andrea C. Ferrari[1]

[1]*Cambridge Graphene Centre, University of Cambridge, 9 JJ Thomson Avenue, CB3 0FA, Cambridge, UK*
[2]*Photonic Networks and Technologies Lab – CNIT, Via G. Moruzzi 1, 56124, Pisa, Italy*
[3]*CamGraPhIC srl, Via G. Moruzzi 1, 56124, Pisa, Italy*
**Now at CamGraPhIC srl*
Author e-mail address: mt840@cam.ac.uk

Abstract: We report graphene electro-absorption modulators on silicon waveguides with 67 GHz electro-optical 3 dB bandwidth, achieving non-return-to-zero optical modulation up to 80 Gb/s in C-band and 40 Gb/s in O-band. © 2026 The Author(s)

1. Introduction

The demand of computational capacity driven by AI requires data centers to improve interconnects bandwidth to reduce latency and maximize throughput, a challenge that can be addressed with integrated photonics transceivers [1]. Graphene (SLG) grown by chemical vapor deposition (CVD) can be integrated on Si waveguides (WGs) at the back-end-of-line [2] and it can provide high bandwidth [3] in useful datacom bands like O- and C-bands [4] in a compact footprint (< 100 μm^2). This is because modulation from visible to mid-infrared is governed by ultrafast (< 3-5 ps [5]) Pauli blocking interband transitions and by charge carrier mobility [2], which can be ~ 10,000 cm^2/Vs for 4” CVD SLG on Cu(111)/sapphire substrates [6]. Therefore, SLG-based dense wavelength division multiplexing transmitters with > 1 $Tb/s/mm^2$ bandwidth density may be possible across both O- and C bands. SLG can also be employed for detectors on the same platform, hence enabling compact transceivers.

Here, we report 40 µm-long wafer-scalable double single-layer graphene (DSLG) electro-absorption modulators (EAMs) on Si WGs with 67 GHz 3 dB bandwidth (BW) and up to 80 Gb/s in C-band and 40 Gb/s in O-band, which correspond to a 30 Gb/s data rate improvement compared to previous scalable demonstrations in C-band [4, 7] thanks to design, material, and fabrication flow optimizations. This showcases SLG as a useful active material for heterogeneous integration on Si photonics platforms for > 1.6 Tb/s applications.

2. Results and discussion

Fig.1.**a** shows C- and O-band devices cross-sections with different WG widths and the electric field profiles calculated in Lumerical MODE at 1550 and 1310 nm, respectively. The double single-layer graphene (DSLG) capacitor is designed for high speed with geometrical parameters shown on Fig.1.**a**. DSLG modulators are fabricated as follows [8]. The first SLG layer is electrochemically delaminated and wet-transferred on a selectively planarized 220 nm silicon-on-insulator (SOI) platform fabricated at CORNERSTONE [8]. After shaping and etching SLG with e-beam lithography and O_2 plasma, hexagonal boron nitride, grown on and transferred from a 2” sapphire wafer, is transferred for protecting SLG from plasma-enhanced atomic layer deposition of Al_2O_3. After a second SLG transfer, metallic contacts are defined by a two-step lithography and thermal evaporation. A first Au contact is defined to overlap with SLG, then a second Cr/Au contact is defined for electrical probing. The O-band mode in Fig.1.**a** is more tightly confined, leading to the reduced optical extinction ratio (*ER*) in simulated optical transmission of a 40 µm-long modulator in Fig.1.**b**. O-band devices have lower maximum static ER (3.6 against 4.8 dB) and higher Pauli blocking threshold, defined by $E_F > hc/2\lambda$ where E_F is the DSLG Fermi level, which is 0.4 eV at 1550 nm and 0.475 eV at 1310 nm. Near the Pauli blocking threshold is where the device should be biased for optimal operation, since *ER/V* is maximized, see Fig.1.**b**. E_F can be converted into $|V-V_{Dirac}|$ using the experimental dielectric constant of the employed gate oxide of thickness t_{ox} = 40 nm, ε_r ~ 6.8 [8]. The voltage, *V*, required to bias the device at the optimal point depends on the DSLG E_F position after fabrication, or V_{Dirac}, which is the voltage required to bring SLG at the charge-neutrality point (0 eV). A typical residual E_F for DSLG on a SiO_2 surface is ~ 0.2-0.3 eV, which for this design corresponds to V_{Dirac} ~ 15-22 V. This leads to V ~ 14 and 8 V in the O-band and C-band, respectively, i.e. a larger bias is required in the O-band due to Pauli blocking. Fig.2.**a** shows static characterization of a 40 µm O-band EAM compared to a 40 µm C-band EAM at 1550 and 1310 nm, confirming the simulations: *ER* ~ 3.5 dB in the C-band and *ER* ~ 2 dB in O.

The ideal bias voltage, i.e. the voltage at which Pauli blocking begins, is ~ 3.5 V in the C-band and ~ -6 V in O, confirming that a higher bias is required at 1310 nm. In Fig.2.**b**, the frequency response is measured with a vector network analyzer (VNA, Keysight PNA N5227B), where port 1 drives the EAM through a 67 GHz RF probe and bias-tee, and port 2 receives the modulated optical signal from a 70 GHz photodiode (Finisar XPD3120R) after optical amplification with an Erbium-doped fiber amplifier (EDFA) and a narrow-band filter. A semiconductor optical amplifier (SOA) is used in the O-band. The 3 dB cut-off frequency, f_{3dB} ~ 67 GHz, is extracted from the calibrated S_{21} curve after correcting for cable, probe, and photodiode response. A simulated S_{21} of the equivalent RC circuit of the modulator is plotted on the same figure, showing good agreement to a model with C = 0.0015 F/m^2 and contact resistance R_C ~ 400 Ωμm. The simulated frequency response suggests ~ 100 GHz 6 dB BW.

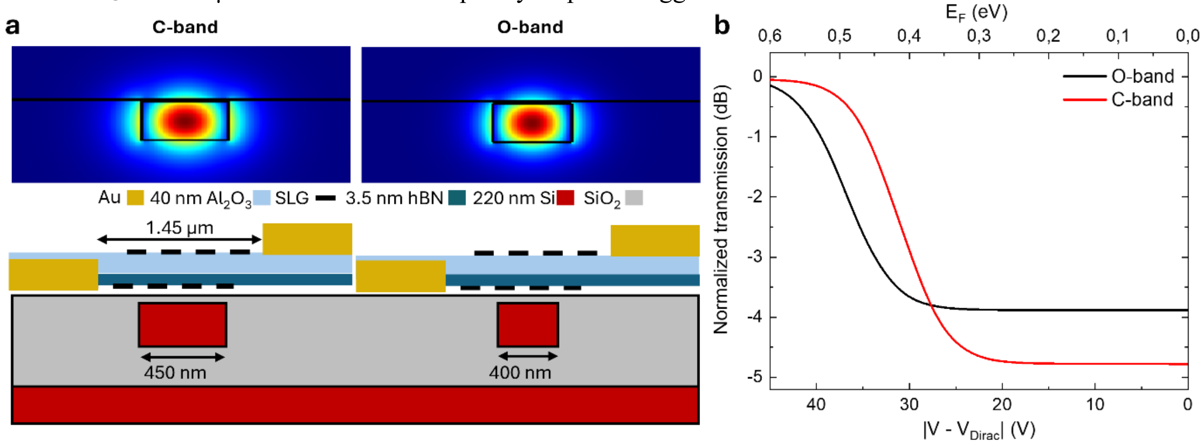

Fig. 1. **a** EAM cross-sections and related electric field profiles for C (1550 nm) and O-band (1310 nm). **b** Simulated optical transmission of a 40 μm-long EAM as a function of bias voltage. This simulation accounts for 5 nm residual SiO_2 cladding on top of Si and a SLG scattering time of 350 fs.

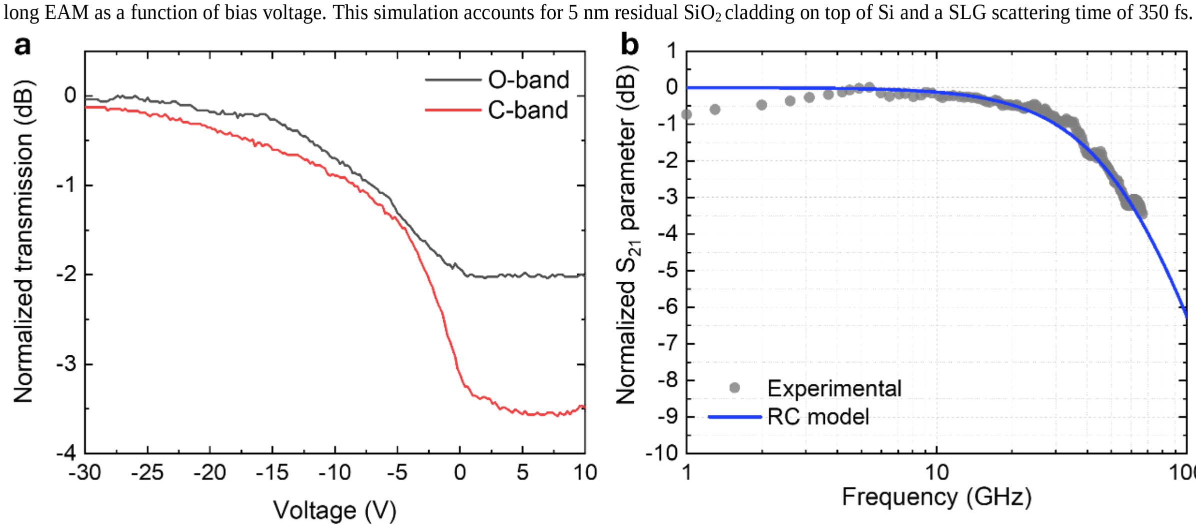

Fig. 2. **a** Experimental static response of O- and C-band EAMs with the same length. **b** Frequency response showing an experimental 67 GHz 3 dB BW and a simulated 100 GHz 6 dB BW.

For the data transmission experiment, port 1 of the VNA is substituted with a 100 Gs digital-to-analog converter (DAC, Micram DAC4) generating pre-emphasized non-return-to-zero (NRZ) signals up to 80 Gb/s. The peak-to-peak output voltage of the DAC is 0.5 V. To increase this, a 50 GHz RF amplifier with 1 dB compression point ~ 20 dBm is used (Centellax UA1L65VM). A 6 dB attenuator is then inserted between the bias tee and the GS probe. This is equivalent to connecting a 50 Ω load to ground, and it is necessary to obtain impedance matching between the amplifier output port and the modulator. A $2^7 - 1$ pseudo-random-binary sequence (PRBS) is prepared and encoded using a NRZ modulation format. This sequence is applied to the EAM, with output fed into a 70 GHz photodiode connected to a 65 GHz sampling oscilloscope, with eye diagrams in Fig.3.**a**,**b**. By monitoring RF losses of the device, bias-tee, probes, and cables, we estimate a peak-to-peak voltage ~ 3 V applied to the EAM, which correspond to < 100 fJ/bit energy consumption. Feed-forward equalization (FFE) and continuous-time linear equalization (CTLE) filtering were applied to flatten the system response and recover clear eye diagrams, from which signal-to-noise ratio (*SNR*), bit error rate (*BER*), and *ER* are extracted and reported in Table 1. *SNR*, and *ER* decrease as data rate increases, leading to higher *BER*, due to increasing noise in the data generation from the DAC.

We achieve a maximum data rate of 80 Gb/s with *ER* ~ 1.41 dB in the C-band and 40 Gb/s with *ER* ~ 0.81 in the O-band. The difference in data rates stems from a combination of weaker electro-optic response in the O-band due to mode confinement and lower optical *SNR*, since the O-band set-up employed a SOA rather than EDFA, yielding a 3 dB lower output power and a higher noise figure (5 dB).

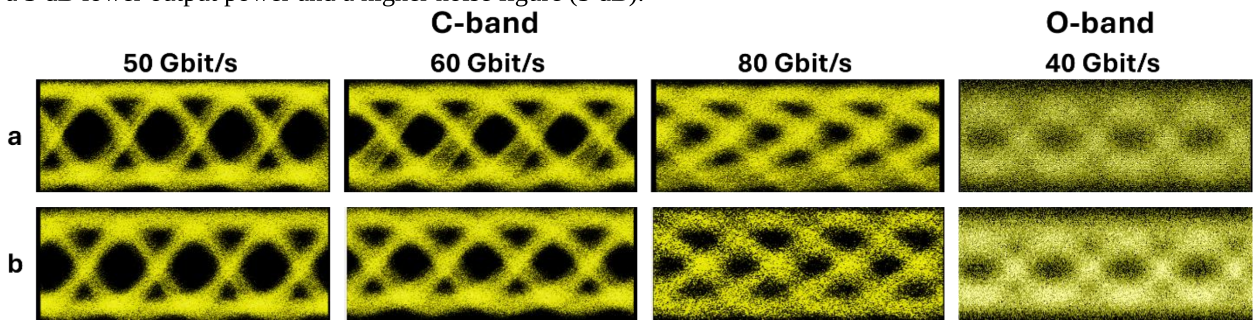

Fig. 3. Eye diagrams of C- and O-band modulators with **a** 40 µm and **b** 100 µm length.

Table 1. Data transmission results extracted from eye diagrams. [a]With pre-emphasis and CTLE filtering.

Band	Length [µm]	NRZ data rate [Gb/s]	SNR	BER	ER [dB]
C	40	50	5.17 [a]	1.2×10^{-7} [a]	1.05 [a]
C	40	60	4.02 [a]	2.9×10^{-5} [a]	1.02 [a]
C	40	80	2.38 [a]	8.5×10^{-3} [a]	0.82 [a]
O	40	40	4.62	4.4×10^{-2}	0.81
C	100	50	4.84 [a]	6.6×10^{-7} [a]	1.89 [a]
C	100	60	3.75 [a]	8.9×10^{-5} [a]	1.74 [a]
C	100	80	2.31 [a]	1×10^{-2} [a]	1.41 [a]
O	100	40	4.81	4.1×10^{-2}	0.81

3. Conclusions

We reported a performance improvement in SLG integrated optical modulators, showing the first 67 GHz 3 dB cut-off BW DSLG EAMs on Si with NRZ data rates of 80 Gb/s in C-band and 40 Gb/s in O-band. For equal designs, we highlighted the superior performance in C-band due to favorable EAM-mode overlap, leading to higher *ER*. However, with minor design changes, such as tapering the O-band WG interacting with SLG and including more SLG layers in the capacitor stack, we expect O-band devices to perform like C-band devices. Both C- and O-band SLG-based modulators can therefore be useful for > 1.6 Tb/s applications.

4. Acknowledgements

We acknowledge funding from EU Graphene Flagship, ERC Grants Hetero2D, GIPT, EU Grants GRAPH-X, CHARM, ELEGANCE, EPSRC Grants EP/K01711X/1, EP/K017144/1, EP/N010345/1, EP/L016087/1, EP/V000055/1, EP/X015742/1, EP/Y035275/1.

References

[1] P. Ossieur, B. Moeneclaey, G. Coudyzer, J. Lambrecht, J. Craninckx, E. Martens, J. Van Driessche, C. Bruynsteen, J. De Busscher, J. Declercq, Y. Gu , S. Niu, T. Pannier, N. Singh, L. Van Severen, L. Bogaert, D. Maes, T. Vanackere, E. Vissers, J. Zhang, S. Kumari, R. Oldenbeuving, X. Zhang , G. Van Elzakker, J. Van Campenhout, P. Absil, B. Kuyken, X. Yin, G. Torfs, J. Missinne, G. Van Steenberge, G. Roelkens and J. Bauwelinck, "Integrated Photonics and Electronics for Optical Transceivers Supporting AI/ML Applications", *IEEE J. Sel. Top. Quantum Electron.* **31**, 6000116 (2025).

[2] M. Romagnoli, V. Sorianello, M. Midrio, F. H. Koppens, C. Huyghebaert, D. Neumaier, P. Galli, W. Templ, A. D'Errico, and A. C. Ferrari, "Graphene- based integrated photonics for next- generation datacom and telecom", *Nat. Rev. Mater.* **3**, 392 (2018).

[3] S. M. Koepfli, M. Baumann, Y. Koyaz, R. Gadola, A. Gungor, K. Keller, Y. Horst, S. Nashashibi, R. Schwanninger, M. Doderer, E. Passerini, Y. Fedoryshyn and J. Leuthold, "Metamaterial graphene photodetector with bandwidth exceeding 500 gigahertz", *Science* **380**, 1169 (2023).

[4] C. Alessandri, I. Asselberghs, S. Brems, C. Huyghebaert, J. Van Campenhout, D. Van Thourhout and M. Pantouvaki, "High speed graphene-silicon electro-absorption modulators for the O-band and C-band", *Jpn. J. Appl. Phys.* **59**, 052008 (2020).

[5] E. A. A. Pogna, A. Tomadin, O. Balci, G. Soavi, I. Paradisanos, M. Guizzardi, P. Pedrinazzi, S. Mignuzzi, K. J. Tielrooij, M. Polini, A. C. Ferrari and G. Cerullo, "Electrically Tunable Nonequilibrium Optical Response of Graphene", *ACS Nano* **16**, 3613 (2022).

[6] Y. Zhu, J. Zhang, T. Cheng, J. Tang, H. Duan, Z. Hu, J. Shao, S. Wang, M. Wei, H. Wu, A. Li, S. Li, O. Balci, S. M. Shinde, H. Ramezani, L. Wang, L. Lin, A. C. Ferrari, B. I. Yakobson, H. Peng, K. Jia and Z. Liu, "Controlled Growth of Single-Crystal Graphene Wafers on Twin-Boundary-Free Cu(111) Substrates", *Adv. Mater.* **36**, 2308802 (2024).

[7] E. Heidari, H. Dalir, F. M. Koushyar, B. M. Nouri, C. Patil, M. Miscuglio, D. Akinwande and V. J. Sorger, "Integrated ultra-high-performance graphene optical modulator" *Nanophotonics*, **11**, 4011 (2022).

[8] M. Tiberi, A. Montanaro, C. Wen, J. Zhang, O. Balci, S. M. Shinde, S. Sharma, A. Meersha, H. Shekhar, J. E. Muench, B. R. Conran, K. B. K. Teo, M. Ebert, X. Yan, Y. Tran, M. Banakar, C. Littlejohns, G. T. Reed, M. Romagnoli, A. Ruocco, V. Sorianello and A. C. Ferrari, "Graphene Electro-Absorption Modulators for Energy-Efficient and High-Speed Optical Transceivers", arXiv:2506.03281 [cond-mat.mtrl-sci] (2025).